Cell Cycle 11:11, 2159-2169; June 1, 2012; © 2012 Landes Bioscience

Phospho-Bcl-x_L(Ser62) plays a key role at DNA damage-induced G_2 checkpoint

Jianfang Wang,[1] Myriam Beauchemin[1] and Richard Bertrand[1,2,*]

[1]Centre de Recherche; Centre Hospitalier de l'Université of Montréal (CRCHUM)-Hôpital Notre-Dame and Institut du Cancer de Montréal; Montréal, QC Canada;
[2]Département de Médecine; Université de Montréal; Montréal, QC Canada

Keywords: Bcl-x_L, cdk1(cdc2), cell cycle checkpoint, DNA damage, nucleolus

Accumulating evidence suggests that Bcl-x_L, an anti-apoptotic member of the Bcl-2 family, also functions in cell cycle progression and cell cycle checkpoints. Analysis of a series of phosphorylation site mutants reveals that cells expressing Bcl-x_L(Ser62Ala) mutant are less stable at the G_2 checkpoint and enter mitosis more rapidly than cells expressing wild-type Bcl-x_L or Bcl-x_L phosphorylation site mutants, including Thr41Ala, Ser43Ala, Thr47Ala, Ser56Ala and Thr115Ala. Analysis of the dynamic phosphorylation and location of phospho-Bcl-x_L(Ser62) in unperturbed, synchronized cells and during DNA damage-induced G_2 arrest discloses that a pool of phospho-Bcl-x_L(Ser62) accumulates into nucleolar structures in etoposide-exposed cells during G_2 arrest. In a series of in vitro kinase assays, pharmacological inhibitors and specific siRNAs experiments, we found that Polo kinase 1 and MAPK9/JNK2 are major protein kinases involved in Bcl-x_L(Ser62) phosphorylation and accumulation into nucleolar structures during the G_2 checkpoint. In nucleoli, phospho-Bcl-x_L(Ser62) binds to and co-localizes with Cdk1(cdc2), the key cyclin-dependent kinase required for entry into mitosis. These data indicate that during G_2 checkpoint, phospho-Bcl-x_L(Ser62) stabilizes G_2 arrest by timely trapping of Cdk1(cdc2) in nucleolar structures to slow mitotic entry. It also highlights that DNA damage affects the dynamic composition of the nucleolus, which now emerges as a piece of the DNA damage response.

Introduction

In mammals, development and tissue homeostasis require a carefully orchestrated balance between cell proliferation, cell differentiation, cellular senescence and cell death. In recent years, several studies have reported that members of the Bcl-2 family, in addition to their central role in controlling apoptosis during development and cellular stress, also interface with the cell cycle, the DNA damage response, DNA repair pathways and premature senescence, effects that are generally distinct from their function in apoptosis.[1,2] Bcl-2 itself has been demonstrated to slow entry from the quiescent G_0 to the G_1 phase of the cell cycle prior to DNA replication in multiple cell lineages and transgenic mice.[3] In contrast, Bcl-$2^{-/-}$-knockout cells enter the S phase more quickly. This effect of Bcl-2 on cell proliferation is genetically distinct from its function in apoptosis.[4] Mcl-1, another Bcl-2 homolog known to function as an anti-apoptotic protein, inhibits cell cycle progression through the S phase of the cell cycle.[5] More recently, others have reported that a proteolytic fragment of Mcl-1 regulates cell growth via interaction with Cdk1(cdc2),[6] and that Mcl-1 plays an essential part in ATR-mediated CHK1 phosphorylation.[7] Others have discerned the involvement of Bid, a BH3-only Bcl-2 family member with pro-apoptotic activity, at the intra-S phase checkpoint under replicative stress in response to DNA damaging agents.[8,9] This function of Bid is mediated through its phosphorylation by the DNA damage signaling kinase ATM.[8,9]

Bcl-2 and/or Bcl-x_L modulate the Rad51-dependent homologous recombination pathway as well as non-homologous end-joining and DNA damage mismatch repair activities, effects that are separable from their anti-apoptotic function.[10-13] Bcl-x_L also fulfills specific functions distinct from its function in apoptosis during the cell cycle.[14-16] Indeed, we previously reported that, in addition to its mitochondrial effect, which delays apoptosis, Bcl-x_L co-localizes in nucleolar structures and binds Cdk1(cdc2) during the G_2 cell cycle checkpoint, and its overexpression stabilizes G_2 arrest in surviving cells after DNA damage induced by DNA topoisomerase I and II inhibitors.[15] Bcl-x_L potently inhibits Cdk1(cdc2) kinase activity, which is reversible by a synthetic peptide between the 41st to 61st amino acids surrounding the described Thr47 and Ser62 phosphorylation sites within its flexible loop domain. A mutant deleted of this region does not alter the anti-apoptotic function of Bcl-x_L but impedes its effect on Cdk1(cdc2) activities and on G_2 arrest after DNA damage.[15] In addition, functional analysis of a Bcl-x_L phosphorylation site mutant, Bcl-x_L(Ser49Ala), has revealed that cells expressing this mutant are less stable at G_2 checkpoint after DNA damage and enter cytokinesis more slowly after microtubule poisoning than cells expressing wild-type Bcl-x_L.[16]

*Correspondence to: Richard Bertrand; Email: richard.bertrand@umontreal.ca
Submitted: 01/12/12; Revised: 05/04/12; Accepted: 05/07/12
http://dx.doi.org/10.4161/cc.20672

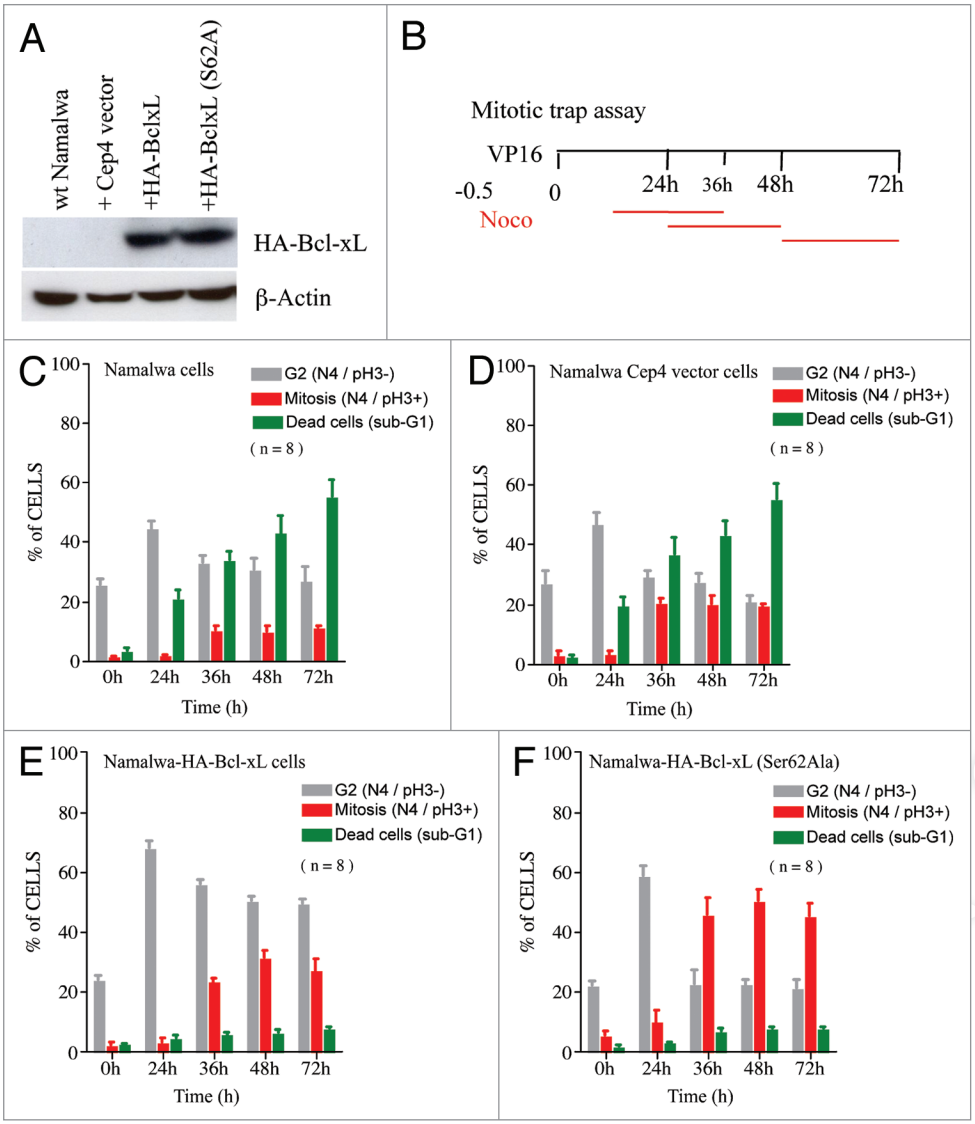

Figure 1. Effect of Bcl-x_L and Bcl-x_L(Ser62Ala) phosphorylation site mutant on DNA damage-induced G_2 arrest. (A) Expression level of HA-Bcl-x_L and HA-Bcl-x_L(Ser62Ala) phosphorylation site mutant in stably transfected Namalwa cell populations. β-actin expression is shown as control. (B) Schematic view of the mitotic trap assay; VP16 was administered at 10 μM for 30 min; nocodazole treatments (0.35 μM) at the indicated intervals trapped cells entering mitosis. (C–F) Kinetics of G_2 arrest [N4 DNA content/phospho-H3 (ser10)-negative cells; gray bars], mitotic slippage [N4 DNA content/phospho-H3 (ser10)-positive cells; red bars] and cell death (sub-G_1 peak; green bars) in wt Namalwa cells and Namalwa cells expressing HA-Bcl-x_L and Bcl-x_L(Ser62Ala) phosphorylation site mutant. Bars represent the means ± SEM of n independent experiments. Data with additional HA-Bcl-x_L phosphorylation site mutants are in **Figures S1 and S2**.

To better understand the importance of the Bcl-x_L flexible loop domain and putative phosphorylation events in regulating Bcl-x_L location and function during the G_2 checkpoint, we generated a series of single-point Bcl-x_L cDNA phosphorylation site mutants, including Thr41Ala, Ser43Ala, Thr47Ala, Ser56Ala, Ser62Ala and Thr115Ala. Among these Bcl-x_L putative phosphorylation sites, Ser62 has been documented as phosphorylated under microtubule poisoning[17] and Th47 and Thr115 following genotoxic stress.[18] Stably transfected cell populations were selected in human B lymphoma Namalwa and cervical carcinoma HeLa cells. In this study, we provide evidence that phospho-Bcl-x_L(Ser62) is a key component in stabilizing DNA damage-induced cell cycle arrest.

Results

Effect of Bcl-x_L and various Bcl-x_L phosphorylation site mutants on DNA damage-induced G_2 cell cycle arrest. To examine the G_2 cell cycle arrest function of Bcl-x_L, we generated various Bcl-x_L phosphorylation site mutants, including Thr41Ala, Ser43Ala, Thr47Ala, Ser56Ala, Ser62Ala and Thr115Ala, then stably expressed them in Namalwa cells (**Fig. 1A; Fig. S1A**). All transfected cell populations showed similar kinetics of cell proliferation. A well-established, simple experimental procedure, referred to as a mitotic trap assay[19] (**Fig. 1B**), evaluated the kinetics of G_2 arrest after DNA damage, the kinetics of mitotic entry after G_2 arrest and the kinetics of cell death. In mitotic trap assay, cells entering mitosis after G_2 arrest, a direct indicator of G_2 checkpoint bypass or checkpoint recovery and adaptation, are trapped by adding a non-toxic (**Fig. S2A**) concentration of nocadazole (0.35 μM) at 24 h intervals in different experiments after etoposide (VP16) treatment (10 μM/30 min in Namalwa cells) and monitored by flow cytometry with phospho-H3(Ser10) labeling (an early mitotic marker) and propidium iodide (PI) staining. Control Namalwa cells (**Fig. 1C**) or Namalwa cells stably transfected with empty vector (**Fig. 1D**) gradually die after exposure to VP16 (sub-G_1 cells; green bars). The apoptotic mode of cell death of Namalwa cells exposed to DNA topoisomerase I and II inhibitors has been well-characterized previously in references 20–25. In contrast, cells stably expressing HA-Bcl-x_L and all phosphorylation site mutants show strong inhibition of apoptosis (**Fig. 1E and F**, sub-G_1 cells, green bars; **Fig. S1C–G**). More than 70% of cells overexpressing wt HA-Bcl-x_L are arrested in G_2 24 h after VP16 treatment [**Fig. 1E**; N4 DNA content and phospho-H3(ser10)-negative cells; gray bars]. However, some of them slowly escape from G_2 and enter early mitosis, 36 to 72 h after VP16 treatment [**Fig. 1E**; N4 DNA content and phospho-H3(ser10)-positive cells; red bars]. Strikingly, cells expressing the phosphorylation mutant

HA-Bcl-x_L(Ser62Ala) enter mitosis much more rapidly and efficiently [**Fig. 1F**; N4 DNA content and phospho-H3(ser10)-positive cells; red bars], revealing that Ser62 is important for Bcl-x_L function at G_2 arrest. Confirmation of these data was made using another mitotic marker, MPM2 immunoreactivity (**Fig. S2B**). In addition, expression of HA-Bcl-x_L(Ser62Ala) has an effect similar to HA-Bcl-x_L in protecting cells from apoptosis (**Fig. 1E and F**; sub-G_1 cells; green bars). Together, these observations suggest that Bcl-x_L's function in cell cycle arrest is distinct from its function in apoptosis, with Ser62 as a key player. The other phosphorylation site mutants, including HA-Bcl-x_L(Thr41Ala), (Ser43Ala), (Thr47Ala), (Ser56Ala) and (Thr115Ala), present a similar phenotype compared with wt HA-Bcl-x_L in terms of G_2 arrest, with only some cells escaping G_2 arrest 36 to 72 h post-VP16 treatment. All of the mutants also show protection from apoptosis (**Fig. S1C–G**). The effects of HA-Bcl-x_L(Ser62Ala) phosphorylation site mutant are similar to the ones described for the Bcl-x_L(Ser49Ala) phosphorylation site mutant.[16] Thus, a double Bcl-x_L(Ser49Ala/Ser62Ala) phosphorylation site mutant has been generated, expressed in Namalwa cells and analyzed (**Fig. S2C**). Unfortunately, the kinetics of cell proliferation expressing the double mutant were reduced in comparaison to wt Namalwa and Namalwa cells expressing HA-Bcl-x_L, HA-Bcl-x_L(Ser49Ala) and HA-Bcl-x_L(Ser62Ala) phosphorylation site mutants, making it difficult to really compare the effects of the double mutant after VP16 treatment (**Fig. S2C**).

HA-Bcl-x_L(Ser62) phosphorylation and location during DNA damage-induced G_2 arrest. HA-Bcl-x_L(Ser62) phosphorylation occurs after VP16 treatment (**Fig. 2A**) in cells undergoing the G_2 checkpoint. A previous study also indicated that endogenous Bcl-x_L co-localized with Cdk1(cdc2) in the nucleolus during the G_2 checkpoint induced by camptothecin (CPT) and VP16 treatment in human cell lines.[15] Thus indirect in cellular inversed and confocal immunofluorescence microscopy was undertaken to monitor the location of wt HA-Bcl-x_L and phosphorylation site mutant HA-Bcl-x_L(Ser62Ala). We observed in Namalwa cells expressing wt

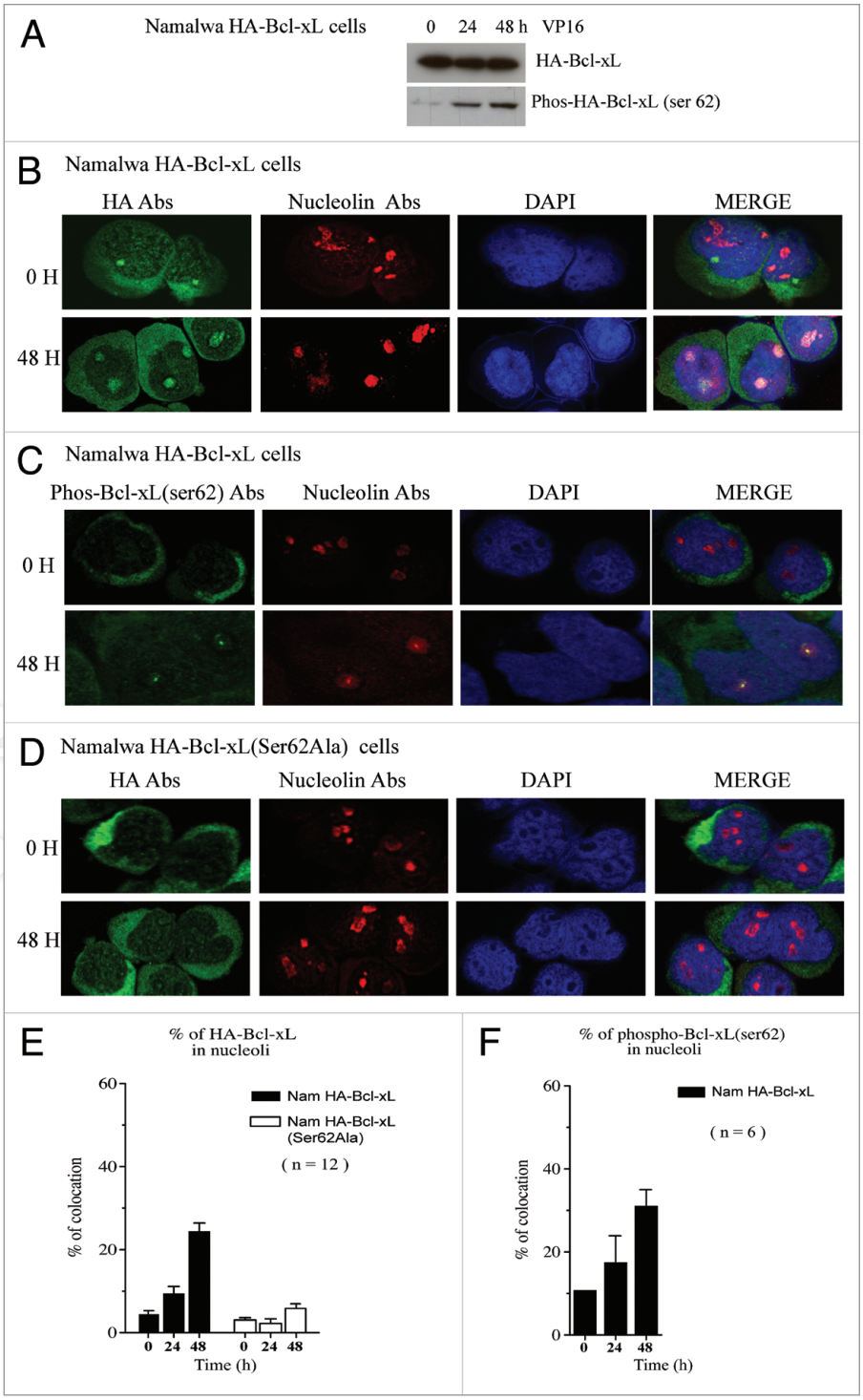

Figure 2. HA-Bcl-x_L(Ser62) phosphorylation and location during DNA damage-induced G_2 arrest. (A) Expression and phosphorylation kinetics of HA-Bcl-x_L after VP16 treatment (10 μM for 30 min). Co-location kinetics of (B) HA-Bcl-x_L and (C) phospho-Bcl-x_L(Ser62) with nucleolin in Namalwa cells expressing HA-Bcl-x_L exposed to VP16 (10 μM for 30 min). (D) Location kinetics of HA-Bcl-x_L(Ser62Ala) and nucleolin in Namalwa cells expressing the phosphorylation site mutant HA-Bcl-x_L(Ser62Ala) exposed to VP16 (10 μM for 30 min). (E) Percentage of HA-Bcl-x_L and HA-Bcl-x_L(Ser62Ala) located in nucleoli in Namalwa cells expressing HA-Bcl-x_L and HA-Bcl-x_L(Ser62Ala) mutant and exposed to VP16 (10 μM for 30 min). Bars represent the means ± SEM from micrographs obtained in *n* independent experiments. (F) Percentage of phospho-Bcl-x_L(Ser62) located in nucleoli in Namalwa cells expressing HA-Bcl-x_L and exposed to VP16 (10 μM for 30 min). Characterization of the phospho-Bcl-x_L(Ser62) antibody preparation is in **Figure S3**.

HA-Bcl-x_L, that a pool of wt HA-Bcl-x_L (**Fig. 2B**) and phospho-Bcl-x_L(ser62) (**Fig. 2C**) co-localized with nucleolin, a marker of the nucleolus, 48 h post-VP16 exposure. In contrast, in Namalwa cells expressing the phosphorylation mutant HA-Bcl-x_L(Ser62Ala) showed no co-location with nucleolin after VP16 treatment (**Fig. 2D**). The percentage of wt HA-Bcl-x_L and phosphorylation mutant HA-Bcl-x_L(Ser62Ala) that co-localized with nucleolin in Namalwa cells was quantified by image analysis (**Fig. 2E**) as well as the percentage of phospho-Bcl-x_L(Ser62) that co-localized with nucleolin in Namalwa cells (**Fig. 2F**). Altogether, these results indicate that phosphorylation at Ser62 is associated with Bcl-x_L accumulation to nucleoli after VP16 treatment, and that accumulation of phospho-Bcl-x_L(Ser62) into nucleoli coincides with the stabilization of G_2 arrest. The specificity of phospho-Bcl-x_L(Ser62) antibodies is depicted in **Figure S3**.

Endogenous Bcl-x_L(Ser62) phosphorylation and location in unperturbed, synchronized cells and during DNA damage-induced G_2 arrest. Because the above observations were made in HA-Bcl-x_L-transfected and overexpressed cells, we next explored the role of endogenous Bcl-x_L in the cell cycle. We performed these experiments in human wt HeLa cells. Indeed, wt HeLa cells are less prone to apoptosis after VP16 treatment and undergo G_2 arrest, with some cells escaping G_2 arrest 48 and 72 h post-VP16 treatment (**Fig. 3A**, left part). Overexpression of Bcl-x_L in HeLa cells also stabilized the G_2 checkpoint (**Fig. 3A**, right part). Bcl-x_L(Ser62) phosphorylation is also seen in untransfected wt HeLa cells exposed to VP16, both in cytosolic- and nuclear-enriched fractions (**Fig. 3B**). When untransfected wt HeLa cells are synchronized by double thymidine block and released, endogenous Bcl-x_L is progressively modified, with accumulation of Ser62 phosphorylation both in cytosolic and nuclear extracts (**Fig. 3C**), indicating that Bcl-x_L phosphorylation on Ser62 occurs during normal cell cycle progression from S phase to G_2 phase of the cell cycle. We next investigated the subcellular location of endogenous phospho-Bcl-x_L(Ser62) in untransfected wt HeLa cells by indirect immunofluorescence staining in asynchronized control and VP16-exposed cells and untreated G_2-synchronized cells (**Fig. 3D–F**). In wt HeLa cells exposed to VP16, phospho-Bcl-x_L(Ser62) accumulated in nucleoli 24 and 48 h post-VP16 exposure. Accumulation in nucleoli was much more marked after VP16 treatment in comparison to synchronized, untreated G_2 cells (**Fig. 3D**). High-resolution and magnification of confocal immunofluorescence micrographs are also presented in **Figure S4** to clearly illustrate co-location of phospho-Bcl-x_L(Ser62) with nucleolin after VP16 treatment, and Z-stacked projections are visualized in **Movies S1 and 2**. Phospho-Bcl-x_L(Ser62) was also found in Cajal bodies with coilin, a specific Cajal body marker, but the location remained unchanged under the conditions tested (**Fig. 3E**). Finally, phospho-Bcl-x_L(Ser62) did not locate in centrosomes with γ-tubulin, a specific centrosome marker (**Fig. 3F**). Taken together, these results indicate that endogenous Bcl-x_L is phosphorylated on Ser62 during normal cell cycle progression, and that phospho-Bcl-x_L(Ser62) accumulates much more strongly in nucleoli during DNA damage-induced G_2 checkpoint in wt HeLa cells, suggesting its importance mostly during DNA damage response.

PLK1 and MAPK9/JNK2 are major protein kinases involved in Bcl-x_L(Ser62) phosphorylation and accumulation in nucleoli during DNA damage-induced G_2 arrest. Various protein kinases have been postulated to phosphorylate Bcl-2 and Bcl-x_L on Ser62 under various experimental conditions, including those driving activation of the mitotic spindle-assembly checkpoint.[17,26-28] No study has yet documented Bcl-x_L phosphorylation on Ser62 at the G_2 checkpoint. Based on an in silico consensus site prediction search (**Table S5**) and on known protein kinases activated during the DNA damage response and G_2 checkpoint, we first tested a part of protein kinases by in vitro kinase assays with recombinant human Bcl-x_L(ΔTM) protein as substrate. Among all the kinases tested, PLK1, MAPK9/JNK2, GSK3α, GSK3β, MAPK8/JNK1, MAPKAPK2 and MAPK14/SAPKp38α were positive and able to phosphorylate recombinant Bcl-x_L(ΔTM) protein on Ser62 in in vitro kinase assays (**Fig. 4A**). The origin of the kinases, kinase assay description and enzyme-specific activities with control substrates are indicated in **Table S3 and Figure S5**. Then, with specific pharmacological inhibitors and VP16-exposed cells, we observed that PLK, JNK and GSK3 inhibitors prevented Bcl-x_L phosphorylation on Ser62 (**Fig. 4B**) in VP16-exposed cells. Deploying a series of specific siRNAs (**Fig. 4C**; see **Table S4 and Fig. S6** for additional information and controls), western blotting of enriched nuclear extracts revealed that the most important kinases involved in Bcl-x_L(Ser62) phosphorylation in G_2-arrested, VP16-treated HeLa cells were PLK1, JNK1, JNK2 and, to a much lesser extent, GSK3β (**Fig. 4D**). Finally, to confirm these results and to monitor the effect of silencing the kinases on phospho-Bcl-x_L(Ser62) accumulation in nucleoli in VP16-exposed cells, indirect in cellular immunofluorescence microscopy was undertaken and quantified (**Fig. 4E**). The data indicate that PLK1 and JNK2 are major protein kinases associated with progressive phospho-Bcl-x_L(Ser62) accumulation in nucleolar structures in VP16-exposed cells. These protein kinases are phosphorylated/activated in wt Hela synchronized cells as cells progress into G_2 (**Fig. S7A**) and in Hela cells treated with VP16 (**Fig. S7B**).

Phospho-Bcl-x_L(Ser62) meets Cdk1(cdc2) in nucleolar structures during DNA damage-induced G_2 arrest. In a series of reciprocal co-immunoprecipitation experiments, endogenous Bcl-x_L protein has been showed to bind to Cdk1(cdc2) during the G_2 checkpoint.[15] Here, taking advantage of the wt and Ser62Ala mutant proteins expressed in Namalwa cells, we repeated some of these experiments on enriched nuclear and enriched nucleolar extracts. In nuclear extracts, we observed that a pool of Bcl-x_L protein co-immunoprecipitating with Cdk1(cdc2) is phosphorylated on Ser62. The phosphorylation mutant Bcl-x_L(Ser62Ala) in nuclear extracts also co-immunoprecipitated with Cdk1(cdc2), but apparently to a lesser extent (**Fig. 5A**). When co-immunoprecipitation experiments were performed on nucleolar extracts (**Fig. 5B**), we noted that phospho-Bcl-x_L(Ser62) co-immunoprecipitated with Cdk1(cdc2), while the phosphorylation mutant Bcl-x_L(Ser62Ala) was not present in nucleolar fractions. Reciprocal co-immunoprecipitation was also undertaken (**Fig. 5B**). Controls on the enriched nuclear and nucleolar fractions are illustrated in **Figure S7C**. These experiments confirmed that phospho-Bcl-x_L(Ser62) accumulated in nucleoli after DNA damage, while

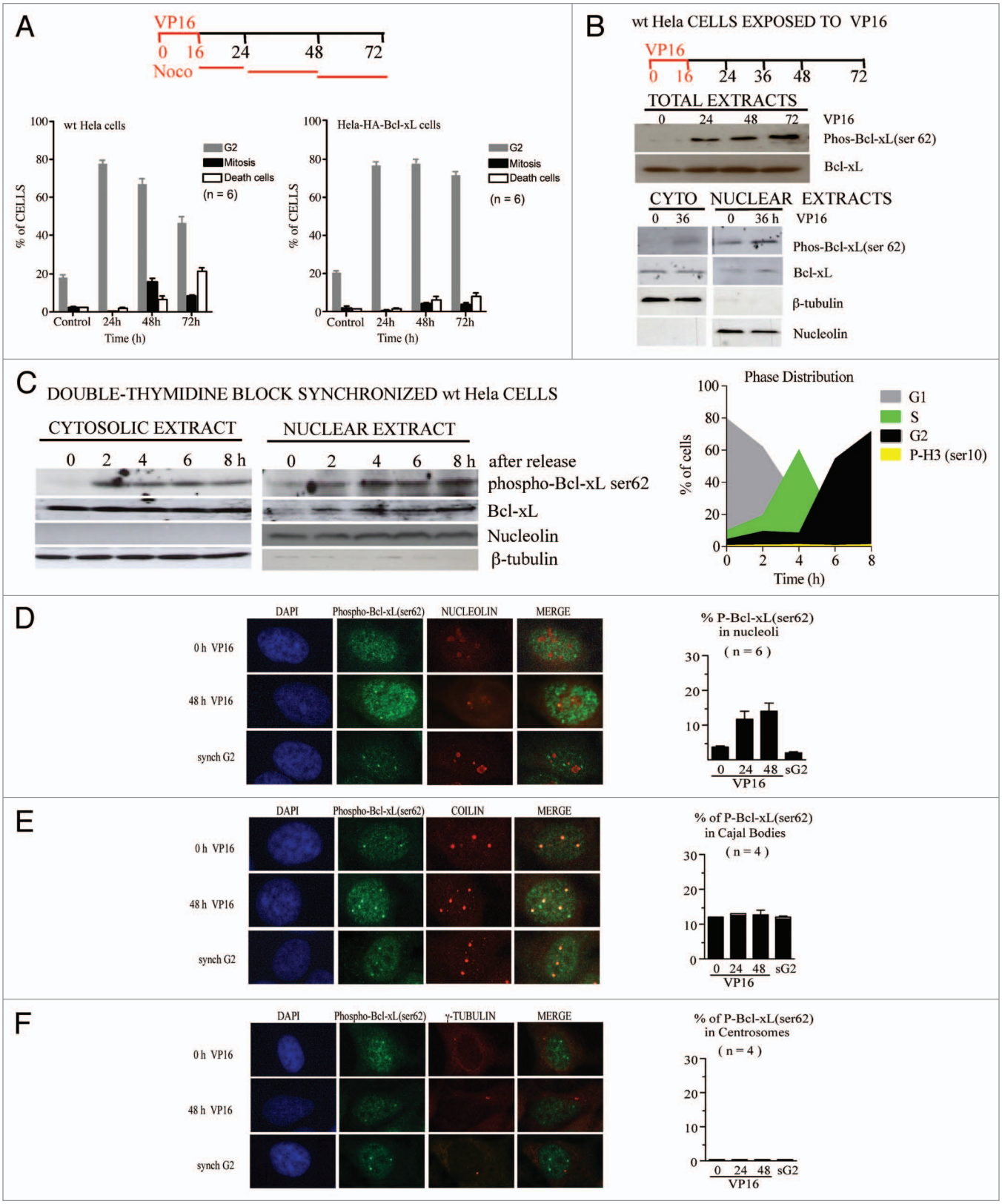

Figure 3. For figure legend, see page 2164.

Figure 3 (See previous page). Endogenous Bcl-x_L(Ser62) phosphorylation and location in unperturbed synchronized HeLa cells and during DNA damage-induced G_2 arrest. (A) wt HeLa cells and HeLa cells expressing HA-Bcl-x_L were exposed to VP16 (10 μM, 16 h), and the kinetics of G_2 arrest (gray bars), mitotic slippage (black bars) and cell death (white bars) were monitored by mitotic trap assay. Bars represent the means ± SEM of six independent experiments. (B) Expression kinetics of endogenous Bcl-x_L and phospho-Bcl-x_L(Ser62) in wt Hela cells exposed to VP16 (10 μM, 16 h). Total protein extracts (upper blots) and proteins obtained from cytosolic and nuclear extracts (lower blots) are shown. Western blots representative of three independent experiments. β-tubulin and nucleolin are cytosolic and nuclear markers. (C) Kinetics of expression of endogenous Bcl-x_L and phospho-Bcl-x_L(Ser62) in synchronized wt Hela cells after double-thymidine block release. Expression levels in cytosolic and nuclear extracts are represented. β-tubulin and nucleolin expression is presented as control. Phase distributions analyzed by flow cytometry with phospho-H3(Ser10) labeling and PI staining are illustrated. Western blots representative of two independent experiments. (D) Co-location kinetics of endogenous phospho-Bcl-x_L(Ser62) with nucleolin (nucleolus marker), (E) coilin (Cajal body marker) and (F) γ-tubulin (centrosome marker) in wt Hela cells exposed to VP16 (10 μM, 16 h) by inversed immunofluorescence microscopy. Percentage of phospho-Bcl-x_L(Ser62) in nucleoli, Cajal bodies and centrosomes during VP16-induced G_2 checkpoint and during normal G_2 phase of the cell cycle in synchronized wt Hela cells (sG_2) are indicated in the right parts. Bars represent the means ± SEM from 12 micrographs obtained in n independent experiments. High-resolution and magnification micrographs obtained by confocal immunofluorescence microscopy and z-stacked projections are in **Figure S4 and Movies S1 and 2**.

the phospho-Bcl-x_L(Ser62Ala) did not. Previous studies also indicated that Bcl-x_L interferes with Cdk1(cdc2) kinase activity in vitro.[15,16] To further investigate the effect of phospho-Bcl-x_L(Ser62) on Cdk1(cdc2) kinase activity, in vitro Cdk1(cdc2) kinase assays were performed in the presence of various amounts of purified recombinant Bcl-x_L(Ser62Asp) protein lacking its C-terminal hydrophobic transmembrane domain (ΔTM). Both wt Bcl-x_L(ΔTM) and Bcl-x_L(Ser62Asp) (ΔTM) inhibited Cdk1(cdc2) activity dose-dependently (**Fig. 5C**). Thus, it appears that Bcl-x_L (Ser62) phosphorylation did not provide advantage compared with the unphosphorylated Bcl-x_L in inhibiting Cdk1(cdc2) kinase activity. Moreover, phospho-Bcl-x_L(Ser62), Cdk1(cdc2) protein and CyclinB1 co-localized with nucleolin in VP16-exposed cells (**Fig. 5D**), whereas the phospho-form of Cdk1(Thr161) did not (**Fig. 5D and E**). High-resolution confocal micrographs are showed in **Figure S4** with Z-stacked projections in **Movies S3 and 4**. Together, the data suggest that during a DNA damage-induced G_2 checkpoint, Bcl-x_L phosphorylation on Ser62 promotes Bcl-x_L accumulation to nucleoli, where it will meet an important pool of Cdk1(cdc2), contributing to its trapping in nucleolar structures to timely avoid entry into mitosis.

Discussion

Our study reveals Bcl-x_L(Ser62) phosphorylation during the normal cell cycle and in DNA damage-induced G_2 arrest. PLK1 and JNK2 are major protein kinases responsible for Bcl-x_L(Ser62) phosphorylation and progressive accumulation in nucleolar structures during the stabilization of DNA damage-induced G_2 arrest. This function of phospho-Bcl-x_L(Ser62) was clearly separable from Bcl-x_L's known purpose in apoptosis, as the Bcl-x_L(Ser62Ala) phosphorylation mutant retained its anti-apoptotic effect but lacked the G_2-arrest stabilization function. This original role of phospho-Bcl-x_L(Ser62) is associated with its accumulation into the nucleolus after DNA damage, where it will meet Cdk1(cdc2). The dynamic complex processes that occur in the nucleolus are emerging.[29] Indeed, the nucleolus acts on cell cycle progression and genomic stability by phased sequestration and the release of regulatory proteins, including p19/ARF, MDM2, CDC14, PP1, p53, telomerase and the DNA helicases WRN and BLM. Cdk1(cdc2) as well as Bcl-x_L or Bcl-2 have also been reported previously in nucleolar structures.[15,30,31] In the nucleolus, phospho-Bcl-x_L(Ser62) binds to and co-localizes with Cdk1(cdc2) in G_2-arrested cells, indicating that it could contribute to the temporal trapping (and inhibition) of Cdk1(cdc2), avoiding unwanted mitosis in the presence of DNA damage. It could also suggest that Bcl-x_L(Ser62) protects nucleolar structures in a timely manner during DNA damage-induced G_2 arrest to avoid rapid nucleolar disassembly associated with mitosis onset. Phospho-Bcl-x_L(Ser62) was also located in Cajal bodies. Although not investigated further in this study, Cajal bodies are known to encompass dynamic trafficking and fusion with nucleolar structures.[29,32] In a recent study, Bcl-x_L(Ser49) phosphorylation has been documented during DNA damage-induced G_2 arrest, with an important pool of phospho-Bcl-x_L(Ser49) accumulating in centrosomes.[16] Thus, it appears that Bcl-x_L contributes to the stabilization of G_2 arrest at least at two specific cellular locations, with phospho-Bcl-x_L(Ser62) at nucleoli and phospho-Bcl-x_L(Ser49) at centrosomes.

Entry into mitosis absolutely requires progressive accumulation of active cyclin B1/Cdk1 (cdc2) complexes in the nucleus. Indeed, recent observations indicate that different levels of cyclin B1/Cdk1(cdc2) kinase activity are organized in a timely manner to coordinate and trigger different mitotic events, the initial activation of cyclin B1/Cdk1(cdc2) complexes occurring about 20 to 25 min before nucleolar disassembly and nuclear envelope breakdown.[33] When cyclin B1/Cdk1(cdc2) activity reaches a specific threshold, it triggers both nucleolar disassembly and nuclear envelope breakdown. After these events, cyclin B1/Cdk1(cdc2) rapidly reaches maximum activity to resume mitosis.[33] Our data suggest that Bcl-x_L(Ser62) phosphorylation is associated with its accumulation to the nucleolus. In the nucleolus, phospho-Bcl-x_L(Ser62) will meet Cdk1(cdc2) during G_2 checkpoint, playing a role in stabilizing G_2 arrest by timely trapping of Cdk1(cdc2) into nucleolar structures to avoid or slow down unwanted mitotic entry. PLK1 activity is regulated both in time and space, and its many functions have also been linked to cell entry into mitosis, centrosomes and microtubule-organizing centers, mitotic exit and cytokinesis.[34] PLK1 accumulates in the nucleus during S and G_2 phases, revealing that it has key functions during the S and G_2 phases of the cell cycle.[35-38] Activation of various MAPK pathways during G_2 and mitosis has also been well documented.[39,40]

Phospho-Bcl-x_L(Ser62) during the normal cell cycle and DNA damage-induced G_2 checkpoint has not previously been documented. Phospho-Bcl-2 and Bcl-x_L(Ser62) has been detected previously in cells treated with microtubule inhibitors, including

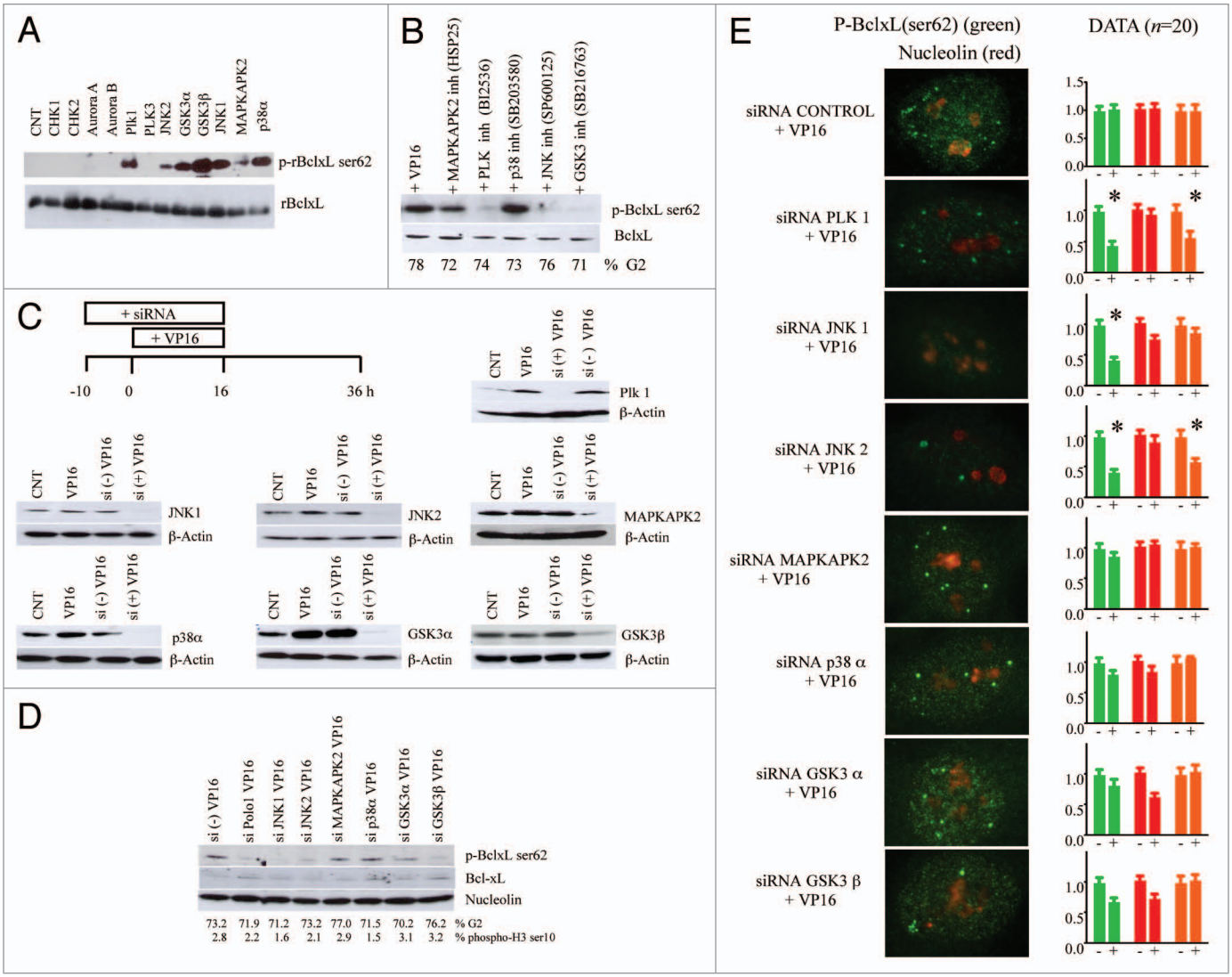

Figure 4. PLK1 and JNK2 are major protein kinases involved in Bcl-x_L(Ser62) phosphorylation and accumulation in nucleoli during DNA damage-induced G_2 arrest. (A) In vitro kinase assays of a part of purified and active protein kinases with recombinant human Bcl-x_L(ΔTM) protein as substrate. All enzyme activities were tested on control substrates (**Fig. S5**). Western blots are representative of four independent experiments. (B) Effects of specific protein kinase inhibitors on Bcl-x_L phosphorylation on Ser62 in Namalwa cells exposed to VP16. Cells were first exposed to VP16 (10 μM, 30 min) and, 12 h post-treatment, kinase inhibitors were added for an additional 12 h: MAPKAPK2 inhibitor (KKA LNR QLG VAA, 10 μM); PLK inhibitor (BI2536, 0.1 μM), p38 inhibitor (SB203580, 2.0 μM), JNK inhibitor (SP600125, 5.0 μM), GSK3 inhibitor (SB216763, 10 μM). Western blots representative of four independent experiments. (C) Effects of specific siRNAs on silencing PLK1, JNK1, JNK2, MAPKAPK2, p38α, GSK3α and GSK3β expression in wt Hela cells. Schematic view of these experiments (C–E) is showed. Additional controls are illustrated in **Figure S6**. (D) Effects of silencing PLK1, JNK1, JNK2, MAPKAP2, p38α, GSK3α and GSK3β expression in wt HeLa cells on the phosphorylation level of endogenous Bcl-x_L(Ser62) after VP16 treatment. Representative western blotting of nuclear extracts of three independent experiments. (E) Co-location of endogenous phospho-Bcl-x_L(Ser62) (green labeling) with nucleolin (red nucleolus labeling) in wt Hela cells exposed to VP16 where various protein kinases are silenced. Quantitation of micrographs obtained by inversed immunofluorescence microscopy is shown in the right parts. Green bars are total phospho-Bcl-x_L(Ser62) staining in cells; red bars are total nucleoli staining in cells; orange bars are the phospho-Bcl-x_L(ser62)/nucleoli staining ratio. Data are presented relative to wt HeLa cells exposed to VP16, and symbols are: (-) cells treated with siRNA control and VP16, (+) cells treated with specific siRNA targeting the given protein kinase and VP16. Bars represent the means ± SEM from 20 micrographs obtained in three independent experiments. *means statistical significance with $p < 0.005$ using two-way Anova (Prism v.5.0d).

nocodazole, paclitaxel, vinblastine and vincristine. Mitotic arrest induced by these compounds is associated with Bcl-2, Bcl-x_L and Mcl-1 phosphorylation. Other studies have revealed that Bcl-2 and Mcl-1 phosphorylation is also tightly coupled with normal mitotic events.[41,42] Multiple kinases have been proposed to phosphorylate Bcl-2 and/or Bcl-x_L at Ser62 in microtubule inhibitor-exposed cells, but most studies have suggested that JNK, normally activated at G_2/M, is one of the protein kinases responsible for Bcl-2 and Bcl-x_L phosphorylation.[18,26-28,43,44]

In summary, our study reveals that PLK1 and JNK2 are major kinases responsible for Bcl-x_L(Ser62) phosphorylation and progressive accumulation in nucleolar structures during stabilization

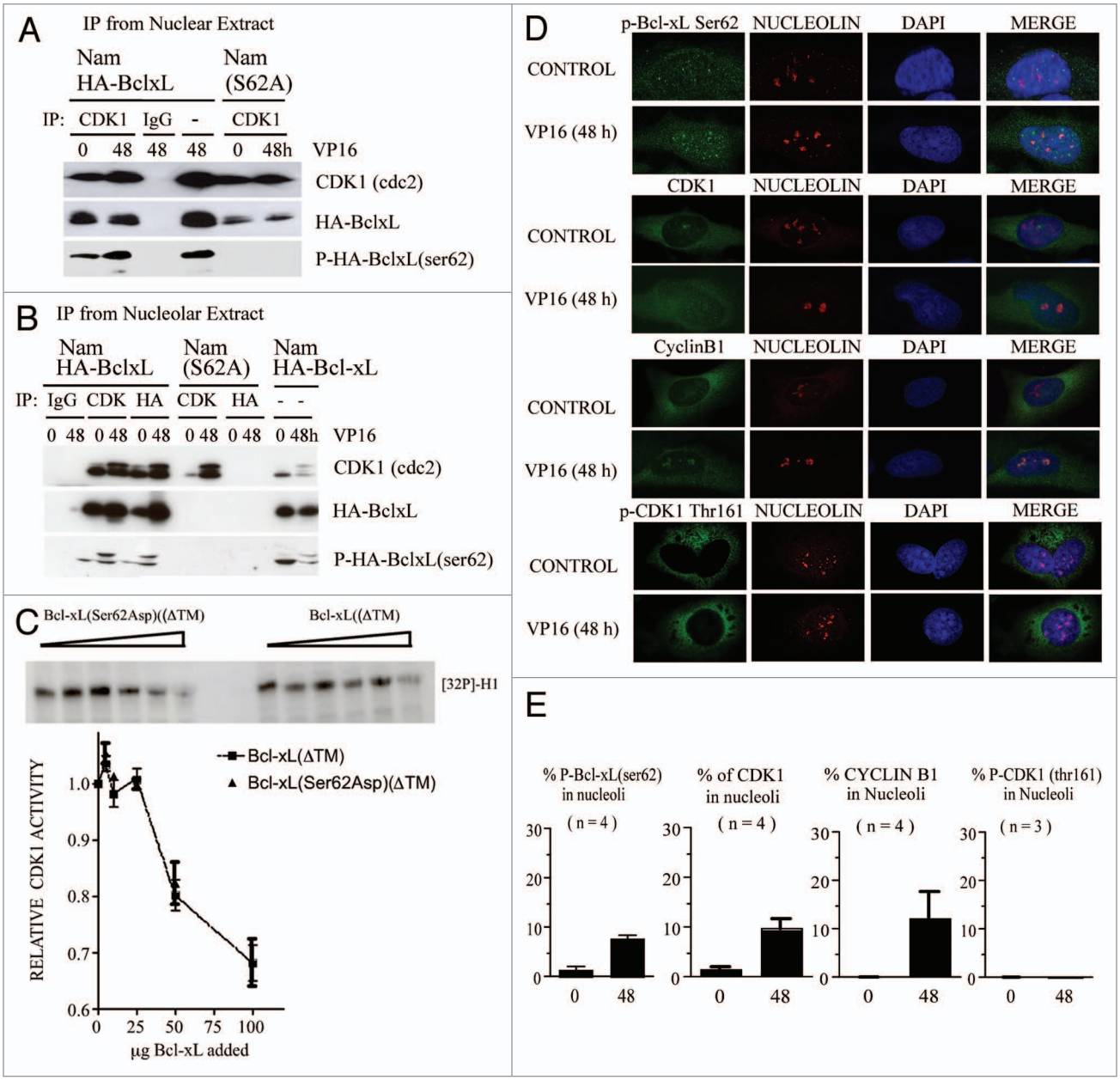

Figure 5. Phospho-Bcl-x_L(Ser62) meets Cdk1(cdc2) in nucleolar structures during DNA damage-induced G_2 arrest. (A) Co-immunoprecipitation of HA-Bcl-x_L, HA-Bcl-x_L(Ser62Ala) and phospho-HA-Bcl-x_L(Ser62) with Cdk1(cdc2) from enriched nuclear extracts obtained from Namalwa cells expressing HA-Bcl-x_L or HA-Bcl-x_L(Ser62Ala) mutant exposed to VP16 (10 µM for 30 min). IgG represents co-immunoprecipitation experiments with control immunoglobulins and (-) indicates a nuclear extract obtained from Namalwa cells expressing HA-Bcl-x_L 48 h post-VP16 treatment loaded as a western blot control. Representative of two independent experiments. (B) Reciprocal co-immunoprecipitation of HA-Bcl-x_L, HA-Bcl-x_L(Ser62Ala) and phospho-Bcl-x_L(Ser62) with Cdk1(cdc2) from enriched nucleolar extracts purified from Namalwa cells expressing HA-Bcl-x_L and HA-Bcl-x_L(Ser62Ala) mutant exposed to VP16 (10 µM for 30 min). IgG, CDK and HA represent co-immunoprecipitation experiments with control immunoglobulins, Cdk1(cdc2) and HA-epitope tag antibodies, respectively. (-) indicates nucleolar extracts obtained from Namalwa cells expressing HA-Bcl-x_L before and after VP16 treatment loaded as western blot controls. Controls on the enriched nuclear and nucleolar fractions are illustrated in **Figure S7C**. (C) In vitro Cdk1(cdc2) kinase activity in the presence of recombinant Bcl-x_L(Ser62Asp)(ΔTM) and Bcl-x_L(ΔTM) proteins. Symbols and bars represent the means ± SEM of six independent experiments. (D) Co-location of phospho-Bcl-x_L(Ser62), Cdk1(cdc2), CyclinB1 and phospho-Cdk1(Thr161) with nucleolin 48 h after VP16 treatment in wt HeLa cells. Inversed immunofluorescence micrographs are representative of three to four independent experiments. (E) Percentage of phospho-Bcl-x_L(Ser62), Cdk1(cdc2), CyclinB1 and phospho-Cdk1(Thr161) with nucleolin in VP16-exposed Hela cells. Bars represent the means ± SEM from micrographs obtained in n independent experiments. Confocal immunofluorescence microscopy analysis and Z-stacked projections are presented in **Figure S4 and Movies S1–4**.

of DNA damage-induced G_2 arrest. It highlights that DNA damage also affects the dynamic composition of a subnuclear domain, the nucleolus, which now emerges as an important piece of the DNA damage cell response.

Materials and Methods

Cell culture, cDNA construction and transfection. Human Namalwa and HeLa cell lines were obtained from the American Type Culture Collection and grown at 37°C under 5% CO_2 in RPMI-1640 medium and DMEM medium supplemented with 10% heat-inactivated fetal bovine serum (FBS), 100 U/ml penicillin and 100 μg/ml streptomycin, respectively. The phosphorylation site mutant cDNAs were generated by triple polymerase chain reactions (PCR) and sub-cloned into pCEP4 and pCDNA3.1 vectors with Kosak consensus sequences and triple HA-tag sequences as described in references 15 and 16. All primers and details are provided in **Table S1**. Transfected cells were grown under hygromycin B1 (pCEP4 vectors) or neomycin (pCDNA3.1 vectors) selection to obtain stable cell population prior to performing the experiments.

Mitotic trap assay and cell synchronization. Mitotic trap assay has been described by Andreassen et al. Briefly cells entering mitosis after G_2 arrest were trapped by adding nocadazole (0.35 μM) at 24 h intervals after VP16 treatment. At the indicated times, the kinetics of G_2 arrest, mitotic entry and cell death were monitored in Coulter EpicsXL flow cytometers with phospho-H3(Ser10) labeling and PI staining or MPM2 labeling with PI staining. HeLa cells were synchronized by double-thymidine block (2 mM) and release.

Protein extraction, subcellular fractionation, immunoblotting and co-immunoprecipitation. To prepare total protein extracts, the cells were extracted with lysis buffer containing 20 mM Hepes(KOH), pH 7.4, 120 mM NaCl, 1% Triton X-100, 2 mM phenylmethylsulfonyl fluoride (PMSF), a cocktail of protease inhibitors (Complete™, Roche Applied Science) and a cocktail of phosphatase inhibitors (PhosStop™, Roche Applied Science). Cytosolic and nuclear extracts were prepared with NE-PER Nuclear and Cytoplasmic extraction reagents according to the manufacturer's protocol (ThermoScientific). Nucleolar fractions were obtained from enriched nuclei according to a procedure adapted from published protocols.[45] Briefly, purified nuclei were re-suspended in 3 ml of 0.34 M sucrose containing 0.5 mM $MgCl_2$ and PhosStop™ and then sonicated on ice for 6 x 6 sec bursts with 10 sec intervals between each burst, with a XL-2000 Microson (Misonix Inc.,) at power setting 5. Nucleoli were then purified by layering the sonicated solution on a 3 ml 0.88 M sucrose cushion containing 0.5 mM $MgCl_2$ followed by centrifugation at 2,000x g for 20 min. Nucleoli pellets were re-suspended in lysis buffer containing 20 mM Hepes(KOH), pH 7.4, 120 mM NaCl, 1% Triton X-100, 0.5% deoxycholate, 2 mM PMSF, a cocktail of protease and phosphatase inhibitors, incubated on ice for 30 min with insoluble materials discarded after centrifugation (10,000x g; 20 min). For immunoprecipitation, samples were first pre-cleaned with a protein A- and G-Sepharose mixture and, after centrifugation, antibodies at 10 μg/ml concentration were incubated at 4°C for 4 h. All antibodies used in this study are listed in **Table S2**. Bcl-x_L(Ser62) antibodies were prepared and purified by GeneScript, using the phosphopeptide-KLH conjugate LAD(phospho-S)PAVNGATGHC as immunogen. The affinity and specificity of the preparation was first analyzed on ELISA, with coated phosphopeptide and non-phosphopeptide as antigens. Further characterization is presented in **Figure S3**.

Protein kinase assays and protein kinase chemical inhibitors. The kinases and kinase assays are described in **Table S3**. Enzyme activities were tested on control substrates, and velocities were expressed as nmole/min/mg (data in **Fig. S5**). Recombinant human Bcl-x_L(ΔTM) and Bcl-x_L(Ser62Asp)(ΔTM) proteins were produced and purified, as described previously in references 15 and 16. The protein kinase chemical inhibitors deployed in this study are listed in **Table S3**.

siRNA-mediated protein kinase inhibition. HeLa cells were transfected with DharmaFECT-1 transfection reagent (ThermoScientific) according to the manufacturer's instructions, with 100 nM of either control siRNA or siRNA targeting different kinases (**Table S4**). The cells were treated 10 h post-transfection with VP16 (10 μM) for 16 h, then washed twice with PBS, followed by their incubation in drug-free medium for an additional 20 h prior to protein extraction and SDS-PAGE.

Immunofluorescence microscopy. Namalwa cells were spread by cytocentrifugation on glass slides, and HeLa cells were seeded and grown directly on coverslips. Both cell types were fixed in methanol at -20°C for 30 min and rapidly immersed into ice-cold acetone for a few seconds. The slides were allowed to dry at room temperature and rehydrated in PBS. Nonspecific binding sites were blocked in PBS containing 5% FBS (blocking solution); then, the slides were incubated sequentially with specific primary antibody (10 μg/ml in blocking solution), specific labeled-secondary antibody (10 μg/ml in blocking solution) followed by DAPI staining, also performed in blocking solution. All antibodies are listed in **Table S2**. Images were generated with a Leica Microsystem mounted on a Leica DM6000B microscope and Leica DFC480 camera hooked up to a MacInctosh computer. All images were quantified with Clemex Vision software (Version 3.0.036, Clemex), as described previously in reference 46. For confocal microscopy analysis, images were generated and analyzed with a Leica TC S SP5 Confocal Microscope mounted with three lasers, Argon, SS561 and HeNe and equipped for spectral imaging and analysis.

Disclosure of Conflicts of Interest

The authors declare no potential conflicts of interest.

Acknowledgments

This work was funded by grant MOP-97913 of the Canadian Institutes of Health Research to R.B. J.W. received scholarships from the China Scholarship Council, the Faculté des études supérieures (Université de Montréal) and the Fondation de l'Institut du cancer de Montréal. The authors thank Dr. Estelle Schmitt (CRCHUM) for her valuable suggestions and the preparation of Bcl-x_L mutant cDNAs. The editorial work of Mr. Ovid Da Silva is appreciated.

Note

Supplemental materials can be found at:
www.landesbioscience.com/journals/cc/article/20672

References

1. Schmitt E, Paquet C, Beauchemin M, Bertrand R. DNA damage response network at the crossroads of cell cycle checkpoints, cellular senescence and apoptosis. J Zhejiang Univ Sci B 2007; 8:377-97; PMID:17565509; http://dx.doi.org/10.1631/jzus.2007.B0377.
2. Danial NN, Gimenez-Cassina A, Tondera D. Homeostatic functions of BCL-2 proteins beyond apoptosis. Adv Exp Med Biol 2010; 687:1-32; PMID:20919635; http://dx.doi.org/10.1007/978-1-4419-6706-0_1.
3. Borner C. Diminished cell proliferation associated with the death-protective activity of Bcl-2. J Biol Chem 1996; 271:12695-8; PMID:8663032.
4. Huang DCS, O'Reilly LA, Strasser A, Cory S. The anti-apoptosis function of Bcl-2 can be genetically separated from its inhibitory effect on cell cycle entry. EMBO J 1997; 16:4628-38; PMID:9303307; http://dx.doi.org/10.1093/emboj/16.15.4628.
5. Fujise K, Zhang D, Liu J, Yeh ET. Regulation of apoptosis and cell cycle progression by MCL1. Differential role of proliferating cell nuclear antigen. J Biol Chem 2000; 275:39458-65; PMID:10978339; http://dx.doi.org/10.1074/jbc.M006626200.
6. Jamil S, Sobouti R, Hojabrpour P, Raj M, Kast J, Duronio V. A proteolytic fragment of Mcl-1 exhibits nuclear localization and regulates cell growth by interaction with Cdk1. Biochem J 2005; 387:659-67; PMID:15554878; http://dx.doi.org/10.1042/BJ20041596.
7. Jamil S, Mojtabavi S, Hojabrpour P, Cheah S, Duronio V. An essential role for MCL-1 in ATR-mediated CHK1 phosphorylation. Mol Biol Cell 2008; 19:3212-20; PMID:18495871; http://dx.doi.org/10.1091/mbc.E07-11-1171.
8. Zinkel SS, Hurov KE, Ong C, Abtahi FM, Gross A, Korsmeyer SJ. A role for proapoptotic BID in the DNA damage response. Cell 2005; 122:579-91; PMID:16122425; http://dx.doi.org/10.1016/j.cell.2005.06.022.
9. Kamer I, Sarig R, Zaltsman Y, Niv H, Oberkovitz G, Regev L, et al. Proapoptotic BID is an ATM effector in the DNA damage response. Cell 2005; 122:593-603; PMID:16122426; http://dx.doi.org/10.1016/j.cell.2005.06.014.
10. Saintigny Y, Dumay A, Lambert S, Lopez BS. A novel role for the Bcl-2 protein family: specific suppression of the RAD51 recombination pathway. EMBO J 2001; 20:2596-607; PMID:11350949; http://dx.doi.org/10.1093/emboj/20.10.2596.
11. Wiese C, Pierce AJ, Gauny SS, Jasin M, Kronenberg A. Gene conversion is strongly induced in human cells by double-strand breaks and is modulated by the expression of BCL-x(L). Cancer Res 2002; 62:1279-83; PMID:11888891.
12. Youn CK, Cho HJ, Kim SH, Kim HB, Kim MH, Chang IY, et al. Bcl-2 expression suppresses mismatch repair activity through inhibition of E2F transcriptional activity. Nat Cell Biol 2005; 7:137-47; PMID:15619620; http://dx.doi.org/10.1038/ncb1215.
13. Wang Q, Gao F, May WS, Zhang Y, Flagg T, Deng X. Bcl2 negatively regulates DNA double-strand-break repair through a nonhomologous end-joining pathway. Mol Cell 2008; 29:488-98; PMID:18313386; http://dx.doi.org/10.1016/j.molcel.2007.12.029.
14. Janumyan YM, Sansam CG, Chattopadhyay A, Cheng N, Soucie EL, Penn LZ, et al. Bcl-x_L/Bcl-2 coordinately regulates apoptosis, cell cycle arrest and cell cycle entry. EMBO J 2003; 22:5459-70; PMID:14532118; http://dx.doi.org/10.1093/emboj/cdg533.
15. Schmitt E, Beauchemin M, Bertrand R. Nuclear colocalization and interaction between bcl-x_L and cdk1(cdc2) during G_2/M cell cycle checkpoint. Oncogene 2007; 26:5851-65; PMID:17369848; http://dx.doi.org/10.1038/sj.onc.1210396.
16. Wang J, Beauchemin M, Bertrand R. Bcl-x_L phosphorylation at Ser49 by polo kinase 3 during cell cycle progression and checkpoints. Cell Signal 2011; 23:2030-8; PMID:21840391; http://dx.doi.org/10.1016/j.cellsig.2011.07.017.
17. Poruchynsky MS, Wang EE, Rudin CM, Blagosklonny MV, Fojo T. Bcl-x_L is phosphorylated in malignant cells following microtubule disruption. Cancer Res 1998; 58:3331-8; PMID:9699663.
18. Kharbanda S, Saxena S, Yoshida K, Pandey P, Kaneki M, Wang Q, et al. Translocation of SAPK/JNK to mitochondria and interaction with Bcl-x(L) in response to DNA damage. J Biol Chem 2000; 275:322-7; PMID:10617621; http://dx.doi.org/10.1074/jbc.275.1.322.
19. Andreassen PR, Skoufias DA, Margolis RL. Analysis of the spindle-assembly checkpoint in HeLa cells. Methods Mol Biol 2004; 281:213-25; PMID:15220532.
20. Schmitt E, Steyaert A, Cimoli G, Bertrand R. Bax-alpha promotes apoptosis induced by cancer chemotherapy and accelerates the activation of caspase 3-like cysteine proteases in p53 double mutant B lymphoma Namalwa cells. Cell Death Differ 1998; 5:506-16; PMID:10200502; http://dx.doi.org/10.1038/sj.cdd.4400376.
21. Schmitt E, Paquet C, Beauchemin M, Dever-Bertrand J, Bertrand R. Characterization of Bax-σ, a cell death-inducing isoform of Bax. Biochem Biophys Res Commun 2000; 270:868-79; PMID:10772918; http://dx.doi.org/10.1006/bbrc.2000.2537.
22. Droin N, Beauchemin M, Solary E, Bertrand R. Identification of a caspase-2 isoform that behaves as an endogenous inhibitor of the caspase cascade. Cancer Res 2000; 60:7039-47; PMID:11156409.
23. Droin N, Rébé C, Bichat F, Hammann A, Bertrand R, Solary E. Modulation of apoptosis by procaspase-2 short isoform: selective inhibition of chromatin condensation, apoptotic body formation and phosphatidylserine externalization. Oncogene 2001; 20:260-9; PMID:11313953; http://dx.doi.org/10.1038/sj.onc.1204066.
24. Paquet C, Schmitt E, Beauchemin M, Bertrand R. Activation of multidomain and BH3-only pro-apoptotic Bcl-2 family members in p53-defective cells. Apoptosis 2004; 9:815-31; PMID:15505424; http://dx.doi.org/10.1023/B:APPT.0000045791.55282.91.
25. Parent N, Sané AT, Droin N, Bertrand R. Procaspase-2S inhibits procaspase-3 processing and activation, preventing ROCK-1-mediated apoptotic blebbing and body formation in human B lymphoma Namalwa cells. Apoptosis 2005; 10:313-22; PMID:15843892; http://dx.doi.org/10.1007/s10495-005-0805-7.
26. Fan M, Goodwin M, Vu T, Brantley-Finley C, Gaarde WA, Chambers TC. Vinblastine-induced phosphorylation of Bcl-2 and Bcl-X_L is mediated by JNK and occurs in parallel with inactivation of the Raf-1/MEK/ERK cascade. J Biol Chem 2000; 275:29980-5; PMID:10913135; http://dx.doi.org/10.1074/jbc.M003776200.
27. Basu A, Haldar S. Identification of a novel Bcl-x_L phosphorylation site regulating the sensitivity of taxol- or 2-methoxyestradiol-induced apoptosis. FEBS Lett 2003; 538:41-7; PMID:12633850; http://dx.doi.org/10.1016/S0014-5793(03)00131-5.
28. Terrano DT, Upreti M, Chambers TC. Cyclin-dependent kinase 1-mediated Bcl-x_L/Bcl-2 phosphorylation acts as a functional link coupling mitotic arrest and apoptosis. Mol Cell Biol 2010; 30:640-56; PMID:19917720; http://dx.doi.org/10.1128/MCB.00882-09.
29. Boulon S, Westman BJ, Hutten S, Boisvert FM, Lamond AI. The nucleolus under stress. Mol Cell 2010; 40:216-27; PMID:20965417; http://dx.doi.org/10.1016/j.molcel.2010.09.024.
30. Barboule N, Truchet I, Valette A. Localization of phosphorylated forms of Bcl-2 in mitosis: co-localization with K_i-67 and nucleolin in nuclear structures and on mitotic chromosomes. Cell Cycle 2005; 4:590-6; PMID:15876860; http://dx.doi.org/10.4161/cc.4.4.1587.
31. Migone F, Deinnocentes P, Smith BF, Bird RC. Alterations in CDK1 expression and nuclear/nucleolar localization following induction in a spontaneous canine mammary cancer model. J Cell Biochem 2006; 98:504-18; PMID:16317763; http://dx.doi.org/10.1002/jcb.20707.
32. Dellaire G, Bazett-Jones DP. Beyond repair foci: subnuclear domains and the cellular response to DNA damage. Cell Cycle 2007; 6:1864-72; PMID:17660715; http://dx.doi.org/10.4161/cc.6.15.4560.
33. Gavet O, Pines J. Progressive activation of CyclinB1-Cdk1 coordinates entry to mitosis. Dev Cell 2010; 18:533-43; PMID:20412769; http://dx.doi.org/10.1016/j.devcel.2010.02.013.
34. Takaki T, Trenz K, Costanzo V, Petronczki M. Polo-like kinase 1 reaches beyond mitosis-cytokinesis, DNA damage response and development. Curr Opin Cell Biol 2008; 20:650-60; PMID:19000759; http://dx.doi.org/10.1016/j.ceb.2008.10.005.
35. Li H, Wang Y, Liu X. Plk1-dependent phosphorylation regulates functions of DNA topoisomerase IIalpha in cell cycle progression. J Biol Chem 2008; 283:6209-21; PMID:18171681; http://dx.doi.org/10.1074/jbc.M709007200.
36. Tsvetkov L, Stern DF. Interaction of chromatin-associated Plk1 and Mcm7. J Biol Chem 2005; 280:11943-7; PMID:15654075; http://dx.doi.org/10.1074/jbc.M413514200.
37. Seki A, Coppinger JA, Jang CY, Yates JR, Fang G. Bora and the kinase Aurora a cooperatively activate the kinase Plk1 and control mitotic entry. Science 2008; 320:1655-8; PMID:18566290; http://dx.doi.org/10.1126/science.1157425.
38. Lobjois V, Jullien D, Bouché JP, Ducommun B. The polo-like kinase 1 regulates CDC25B-dependent mitosis entry. Biochim Biophys Acta 2009; 1793:462-8; PMID:19185590; http://dx.doi.org/10.1016/j.bbamcr.2008.12.015.
39. Manke IA, Nguyen A, Lim D, Stewart MQ, Elia AE, Yaffe MB. MAPKAP kinase-2 is a cell cycle checkpoint kinase that regulates the G_2/M transition and S phase progression in response to UV irradiation. Mol Cell 2005; 17:37-48; PMID:15629715; http://dx.doi.org/10.1016/j.molcel.2004.11.021.
40. Oktay K, Buyuk E, Oktem O, Oktay M, Giancotti FG. The c-Jun N-terminal kinase JNK functions upstream of Aurora B to promote entry into mitosis. Cell Cycle 2008; 7:533-41; PMID:18431843; http://dx.doi.org/10.4161/cc.7.4.5660.
41. Ling YH, Tornos C, Perez-Soler R. Phosphorylation of Bcl-2 is a marker of M phase events and not a determinant of apoptosis. J Biol Chem 1998; 273:18984-91; PMID:9668078; http://dx.doi.org/10.1074/jbc.273.30.18984.

42. Scatena CD, Stewart ZA, Mays D, Tang LJ, Keefer CJ, Leach SD, et al. Mitotic phosphorylation of Bcl-2 during normal cell cycle progression and Taxol-induced growth arrest. J Biol Chem 1998; 273:30777-84; PMID:9804855; http://dx.doi.org/10.1074/jbc.273.46.30777.
43. Maundrell K, Antonsson B, Magnenat E, Camps M, Muda M, Chabert C, et al. Bcl-2 undergoes phosphorylation by c-Jun N-terminal kinase/stress-activated protein kinases in the presence of the constitutively active GTP-binding protein Rac1. J Biol Chem 1997; 272:25238-42; PMID:9312139; http://dx.doi.org/10.1074/jbc.272.40.25238.
44. Yamamoto K, Ichijo H, Korsmeyer SJ. BCL-2 is phosphorylated and inactivated by an ASK1/Jun N-terminal protein kinase pathway normally activated at G(2)/M. Mol Cell Biol 1999; 19:8469-78; PMID:10567572.
45. Ochs RL. Methods used to study structure and function of the nucleolus. Methods Cell Biol 1998; 53:303-21; PMID:9348514; http://dx.doi.org/10.1016/S0091-679X(08)60884-5.
46. Parent N, Winstall E, Beauchemin M, Paquet C, Poirier GG, Bertrand R. Proteomic analysis of enriched lysosomes at early phase of camptothecin-induced apoptosis in human U-937 cells. J Proteomics 2009; 72:960-73; PMID:19393779; http://dx.doi.org/10.1016/j.jprot.2009.04.003.